

Effect of random impurity distribution on the luminescence of n - i - p - i doping superlattices

M. Renn, C. Metzner, and G. H. Döhler

*Institut für Technische Physik I, Universität Erlangen,
Erwin-Rommel-Strasse 1, Erlangen, Federal Republic of Germany*

(Received 9 February 1993)

The experimentally observed luminescence spectra of n - i - p - i doping superlattices composed of uniformly doped n - and p -type layers are much broader than the theoretically calculated ones obtained if a strictly two-dimensional (2D) steplike density of states is assumed. In this paper we demonstrate that surprisingly good agreement between theoretical and experimental spectra is obtained if a broadening of the 2D density of states caused by the spatial potential fluctuations is taken into account in an appropriate way. Our approach for including the random distribution of the impurities resembles the Kane model and is free of fitting parameters.

I. INTRODUCTION

Most of the properties of doping superlattices (DSL's) (Refs. 1 and 2) can be explained in terms of a quasi-two-dimensional (Q2D) electronic band structure resulting from the periodic modulation of the conduction and valence band due to a periodic space charge potential which changes its strength as a function of the degree of excitation, i.e., the spatially separated free electrons and holes in the layers (Fig. 1). For the sake of simplicity the fact that the carriers reside in regions that are strongly perturbed by the presence of the impurities has usually been neglected. The potential fluctuations due to randomly distributed charged impurities lead to a broadening of the electronic subbands. These effects can be quite large in doping superlattices, since the doping levels are typically high and the potential fluctuations caused by the impurity atoms are only partially compensated by mobile carriers of opposite sign, in contrast to (uniformly) doped bulk semiconductors. The situation can become extreme in the ground state of a doping superstructure or in the case of low excitation where the potential fluctuations are nearly unscreened like in a compensated doped bulk semiconductor. Therefore, one expects that the electronic states are not only localized with respect to the direction of the superstructure, but they may also be localized within the plane and the momentum parallel to the layers \mathbf{k}_{\parallel} may no longer be a good quantum number. Although the formation of 2D subbands is expected at sufficiently high excitation levels and has been demonstrated in Raman spectroscopy,³ tunneling,⁴ and magnetotransport⁵ investigations they could not be observed in luminescence experiments on doping superlattices consisting of uniformly doped layers. There have, however, been several reports by Schubert and co-workers^{6,7} on luminescence and absorption experiments in very strongly doped short period δ - n - i - p - i structures where the structure of the spectra could be correlated to electronic subbands.

From the results of previous investigations on three- and two-dimensional impurity systems,^{8,9} it is clear that

for high doping levels the impurity band merges with the neighboring conduction or valence band. In this case the effect of the fluctuations can be well described by means of band tails. The shape of the band tails depends on the screening. Here n - i - p - i structures represent an ideal system, because the free carrier concentration and so the screening can be varied within a wide range.^{10,11}

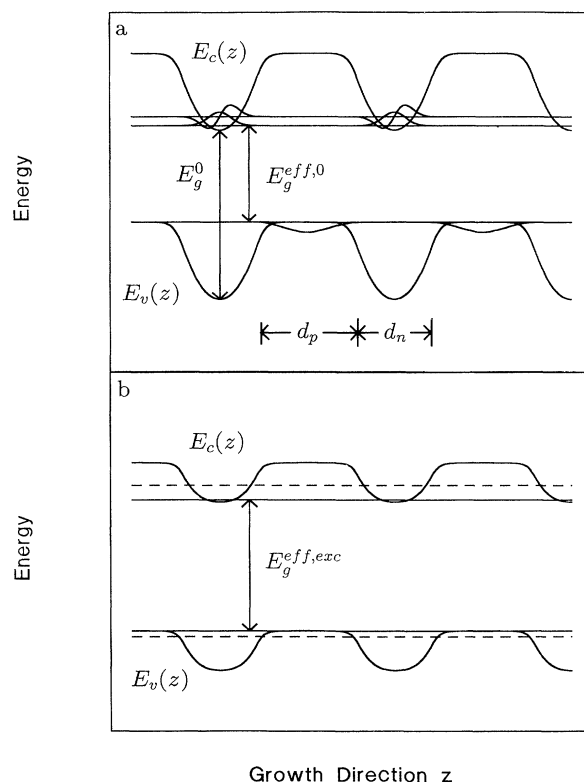


FIG. 1. Ground state (a) and one excited state (b) of the investigated n - i - p - i structure, including the energy levels and wave functions of two conduction and one valence band. The two dashed horizontal lines in part (b) represent the quasi-Fermi-levels Φ_n and Φ_p .

In the case of *n-i-p-i*-structures Bruno and Ruden¹² could show that the random distribution of charged impurities leads to a broadening of the acceptor impurity band which exceeds the acceptor binding energy already at low doping densities of about 10^{18} cm^{-3} . In this paper we demonstrate once more the necessity to include the fluctuations in the calculation of luminescence spectra and present a simple model for their description. The results are discussed in comparison with experimental photoluminescence spectra.

II. EXPERIMENT

The GaAs DSL investigated in the experiments was grown by molecular beam epitaxy (MBE) and consists of 10 *n*- (Si doped) and 11 *p*- (Be doped) layers, with the following parameters: $n_D = 4 \times 10^{18} \text{ cm}^{-3}$, $n_A = 10^{19} \text{ cm}^{-3}$, $d_n = 25 \text{ nm}$, and $d_p = 35 \text{ nm}$. This *p-n...p* structure has cladding layers of undoped $\text{Al}_{0.3}\text{Ga}_{0.7}\text{As}$.

The photoluminescence (PL) measurements were carried out at $T = 90 \text{ K}$. For excitation a Ti-sapphire laser pumped by an argon laser was driven at the wavelength $\lambda = 750 \text{ nm}$. At this wavelength the excitation densities at the first and last superlattice layer differ by about a factor of 2. The excitation density was changed by the use of neutral density filters in the range from 0.03 to 1000 W/cm^2 . The PL spectra, shown in Fig. 2, are measured with a typical setup, using a liquid nitrogen cooled germanium detector, because of the strongly redshifted luminescence of *n-i-p-i* structures at low excitation levels. The spectra were corrected to the spectral response of the optical system.

III. THEORY OF THE LUMINESCENCE AT FINITE TEMPERATURE

A. Without broadening effects

We start with the quantum states of the mobile carriers calculated using a self-consistent solution of the Poisson and Schrödinger equation. Details of this finite temperature Hartree calculation in the effective mass approxi-

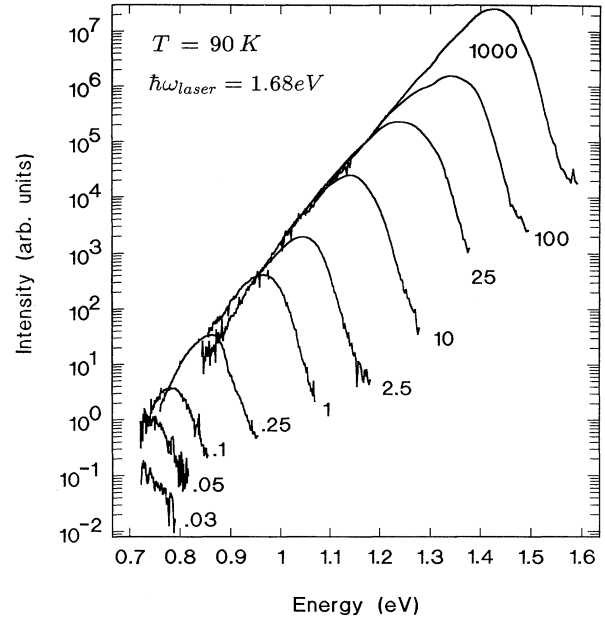


FIG. 2. Photoluminescence spectra for various excitation densities in W/cm^2 , as assigned to the curves. The effective band gap in the ground state $E_g^{\text{eff},0}$ is about 800 meV.

mation can be found in Ref. 13 and will not be repeated. The quantum states are characterized by the carrier type (el, lh, hh), the subband index ($\mu, \nu = 0, 1, 2, \dots$), and the wave vector (\mathbf{k}_{\parallel}). The envelope wave functions $|\text{el}, \mu\rangle$ and $|h, \nu\rangle$ and energy levels E_{μ}^{el} and E_{ν}^h have to be calculated separately for each excitation level, as the modulation of the conduction and valence band changes with carrier concentration due to the changing compensation of impurity space charge.

Now these quantum states are used to calculate the rate of spontaneous radiative recombination of electrons and holes,¹³ neglecting the photon wave vector (conservation of \mathbf{k}_{\parallel}) and averaging over the different polarizations. The number of photons of energy $\hbar\omega$, emitted spontaneously per time interval, is given by the expression

$$R_{\text{spont}}(\hbar\omega) \propto \sum_{h=\text{lh, hh}} |P_{\text{el}, h}|^2 \sum_{\mu\nu} |\langle \text{el}, \mu | h, \nu \rangle|^2 \frac{M_{\text{el}, h}}{2\pi\hbar^2} \Theta[\hbar\omega - (E_{\mu}^{\text{el}} - E_{\nu}^h)] f_n(1 - f_p), \quad (1)$$

with

$$f_n = f\left(E_{\mu}^{\text{el}} + \frac{M_{\text{el}, h}}{m_{\text{el}}} [\hbar\omega - (E_{\mu}^{\text{el}} - E_{\nu}^h)] - \Phi_n\right)$$

and

$$f_p = f\left(E_{\nu}^h + \frac{M_{\text{el}, h}}{m_h} [\hbar\omega - (E_{\mu}^{\text{el}} - E_{\nu}^h)] - \Phi_p\right). \quad (2)$$

Here $P_{\text{el}, h}$ is the bulk interband matrix element of the momentum operator, $\frac{M_{\text{el}, h}}{2\pi\hbar^2} \Theta(\dots)$ is the steplike joint 2D

density of states (2D-DOS) with the reduced effective mass $(M_{\text{el}, h})^{-1} = m_{\text{el}}^{-1} + m_h^{-1}$, $f(\epsilon) = (e^{\epsilon/kT} + 1)^{-1}$ is the Fermi distribution function, and Φ_n, Φ_p are the quasi-Fermi-levels of electrons and holes, respectively.

The recombination rate R_{spont} is dominated by the overlap matrix element of the electron and hole envelope functions $\xi_{\mu}^{\text{el}}(z) \equiv \langle z | \text{el}, \mu \rangle$ and $\xi_{\nu}^h(z) \equiv \langle z | h, \nu \rangle$, because they are separated in real space with respect to the z direction (see Fig. 1). The matrix elements increase strongly for higher energy levels and higher excitation levels, because the corresponding envelope functions are more extended.

Figure 3 shows a comparison between an experimentally observed and a theoretical spectrum for $T = 90$ K calculated by using Eq. (1). The design parameters used in the calculation are those given in Sec. II. The excitation level was chosen such that theoretical and experimental spectra have the same peak position. The high energy tail is well described by the theory, thus confirming the assumption that the thermalized mobile carriers have approximately the same temperature as the host lattice. It should be pointed out that this tail is flatter than expected from a simple $\exp(-\hbar\omega/kT)$ law, because of the increasing overlap matrix elements. At the low energy side the theoretical spectrum is cut off at the lowest possible transition. The discrepancies to the experimental spectra which exhibit a wide low energy tail and no subband structure are obvious. The nonuniform excitation of the layers, mentioned in the previous section, leads to a broadening of about 30 meV of the spectra, because of the superposition of the luminescence of each layer. This effect is too small to explain the observed broadening and does not lead to an exponential low energy tail. The resulting spectra are also cut off with the lowest possible transition of the lowest excited (i.e., the deepest) layer.

In the next section we will show that this low energy tail and the disappearance of the subband structure can be explained by including the effect of the potential fluctuations into the theory.

B. With broadening effects included

1. General considerations

It is clear that the periodic modulation of the conduction- and valence-band edges shown in Fig. 1 de-

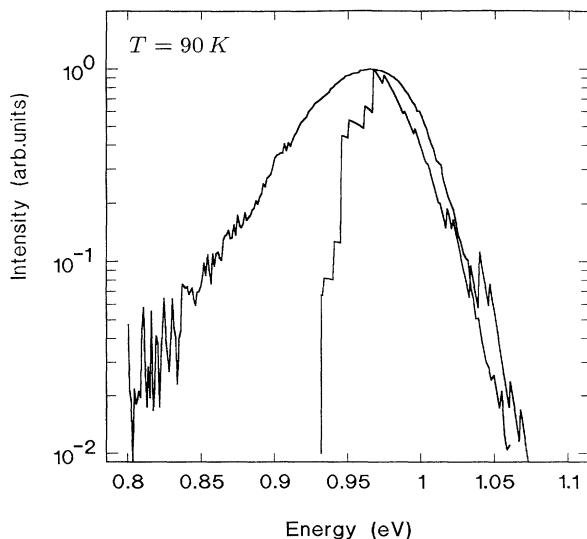


FIG. 3. Calculated spectrum resulting from the theory with no broadening effects for an electron sheet density of $n^{(2)} = 1.2 \times 10^{12} \text{ cm}^{-2}$ in comparison with a corresponding experimental spectrum.

scribes only the mean contribution of the impurities to the space charge potential. The random distribution of the impurities within the doping layers leads to a spatially fluctuating variation of this mean potential. If there are carriers in the layers the potential fluctuations are screened to some extent. Here the first problem arises as the carrier distribution is nonuniform with respect to the z direction. Therefore in a semiclassical picture, the local screening length changes as a function of z . Moreover, the carrier density for a given value of z may fluctuate significantly within the (x, y) direction, due to the random distribution of the impurity atoms. This effect is particularly pronounced at low carrier densities.

The electronic states in this partially screened random potential, of course, will differ from the unperturbed subband states, characterized by the quantized motion in the z direction and the wave vector \mathbf{k}_{\parallel} of free motion parallel to the layers, with regard to both energy eigenvalues E_{μ}^{el} or E_{ν}^h and wave functions.

In particular, we expect that the eigenstates in the low energy tail of the density of states are strongly localized. It should be pointed out that while being localized within the plane, the corresponding wave functions are also more strongly localized in the z direction as compared to those obtained for the idealized mean impurity potential. This will turn out to be important for the calculation of luminescence spectra in real systems with fluctuations. With increasing energy and with increasing carrier density at higher excitation the states become increasingly less localized. Finally, the higher energy states will become delocalized or only weakly localized. But also for these states \mathbf{k}_{\parallel} may not yet be a good quantum number.

Thus, the calculation of the real density of states and the corresponding wave functions as a function of increasing carrier density is a serious problem which has not yet been solved in a satisfactory way.

The next step, the calculation of the luminescence spectra, becomes even more difficult, as the \mathbf{k}_{\parallel} selection rules no longer apply. The overlap integrals $\langle h, \nu | \text{el}, \mu \rangle$ in Eq. (1) have to be replaced by those corresponding to the real states. This leads to the consideration of complicated averaging processes in real and energy space.

Up to now we do not have an exact theory, which takes all these points into account. In a luminescence experiment one always gets the mean effect of the fluctuations on the spectrum according to the large observation area. So, a first step towards a more realistic description of the luminescence may be a model, which takes the randomness into account only by considering statistically fluctuating electric energy levels, but leaving the wave functions unchanged.

2. Modified Kane model

The well known Kane model¹⁴ describes how the 3D-DOS has to be modified to include the effect of doping-induced disorder in a semiclassical way:

$$\bar{D}^{(3)}(E) = \int_{-\infty}^{+\infty} dV P(V, \Delta V) D^{(3)}(E - V). \quad (3)$$

Here $P(V, \Delta V)$ is a probability distribution for the local shift of the 3D-DOS, characterized by the fluctuation width ΔV (see Fig. 4), and the density of states $D^{(3)}(E)$ is

$$D^{(3)}(E) = \frac{1}{2\pi^2} \left(\frac{2m_e}{\hbar^2} \right)^{3/2} (E - E_c)^{1/2} \Theta(E - E_c). \quad (4)$$

To apply a modified Kane model to the 2D systems in a n - i - p - i structure, we made the following simplifying assumptions.

(i) The potential fluctuations in the n and p layers are uncorrelated.

(ii) The screening length is assumed as independent of the position coordinate z . Its value corresponds to that for bulk material, as the classical thickness of the neutralized layers is usually significantly larger than the screening lengths, which indicates that the screening is quasi-three-dimensional. This 3D screening length L_i is given by

$$L_i^2 = \frac{\varepsilon \varepsilon_0 \hbar^2 \pi}{e^2 \bar{m}_i} \left(\frac{\pi}{3\bar{n}_i} \right)^{1/3}, \quad i = \text{el, lh, hh}, \quad (5)$$

within the linearized Thomas-Fermi approximation for degenerate semiconductors. The average effective masses \bar{m}_i are defined as $\bar{m}_{\text{el}} = m_{\text{el}}$ in the case of electrons and as $\bar{m}_{\text{lh}} = \bar{m}_{\text{hh}} = (m_{\text{hh}}^{3/2} + m_{\text{lh}}^{3/2})^{2/3}$ in the case of holes. For the 3D free carrier density \bar{n}_i we take the mean value for a uniform distribution of the excited 2D-carrier concentration $n^{(2)}$ over the width d of the respective layers:

$$\bar{n}_i = \begin{cases} n^{(2)}/d_n, & i = \text{el} \\ p^{(2)}/d_p, & i = \text{lh, hh}. \end{cases} \quad (6)$$

(iii) The overlap matrix elements are chosen to be constant for each subband pair combination and no reduc-

tion or enhancement according to the fluctuations is assumed. This means that we only consider fluctuations parallel to the layers and neglect those in the z direction.

Kane used for the probability distribution $P(V, \Delta V)$ in Eq. (3) a Gaussian distribution:

$$P_G(V, \Delta V_G) = (\sqrt{2\pi} \Delta V_G)^{-1} e^{-\frac{1}{2}(V/\Delta V_G)^2}, \quad (7)$$

with

$$\Delta V_G = \frac{e^2}{4\pi\varepsilon\varepsilon_0} (2\pi n_D L_{\text{el}})^{1/2}, \quad (8)$$

where n_D is the 3D bulk doping density and L_{el} the electronic screening length of the n semiconductor. This is the result that one gets by evaluating the Holtsmark formula¹⁵ to the second order. For details we refer to the Appendix.

Unger¹⁶ pointed out that the Gaussian distribution is only applicable for high doping concentrations n_D , according to

$$n_D L_{\text{el}}^3 \gg 1. \quad (9)$$

This is far beyond normal doping levels [we note that $n_D L_{\text{el}}^3 = 1$ for (uncompensated) n semiconductors is obtained for a doping level of $n_D = 1.5 \times 10^{19} \text{ cm}^{-3}$ and analogously $n_A = 2.8 \times 10^{20} \text{ cm}^{-3}$ for p semiconductors using Eq. (5)]. Another reason for not applying the Gaussian distribution is that it does not produce an exponential tail on the low energy side of the luminescence spectra, as always observed in the case of bulk material. This is also confirmed by a calculation of Halperin and Lax,¹⁷ who found a shape proportional to $\exp(-a|E|^m)$ with increasing $m = 1/2, \dots, 2$ for increasing concentrations. Using this result, we again estimate $m = 1$ for concentrations of interest to us. To take these points into account, Unger chose an empirical distribution, which is proportional to the derivative of a Fermi function and decays more slowly. This has the additional advantage that all appearing integrals are easy to handle in terms of Fermi integrals,¹⁸

$$P_U(V, \Delta V_i) = \frac{1}{\Delta V_i [1 + \exp(+V/\Delta V_i)] [1 + \exp(-V/\Delta V_i)]}. \quad (10)$$

The width ΔV_i of this distribution is given by

$$\Delta V_i = \frac{\sqrt{2}}{2.565} \frac{e^2}{4\pi\varepsilon\varepsilon_0} (2\pi n_i^{\text{dop}} L_i)^{1/2}, \quad i = \text{el, lh, hh}, \quad (11)$$

where $n_{\text{el}}^{\text{dop}} = n_D$, $n_{\text{lh}}^{\text{dop}} = n_{\text{hh}}^{\text{dop}} = n_A$, and L_i is the screening length defined in Eq. (5). This expression leads to the same half-width at full maximum as for the Gaussian distribution.

The broadening of the 2D-DOS is carried out similarly to the case of the Kane model by replacing the 3D- by the 2D-DOS in Eq. (3):

$$\bar{D}_i^{(2)}(E) = \int_{-\infty}^{+\infty} P_U(V, \Delta V_i) D_i^{(2)}(E - V), \quad i = \text{el, lh, hh}, \quad (12)$$

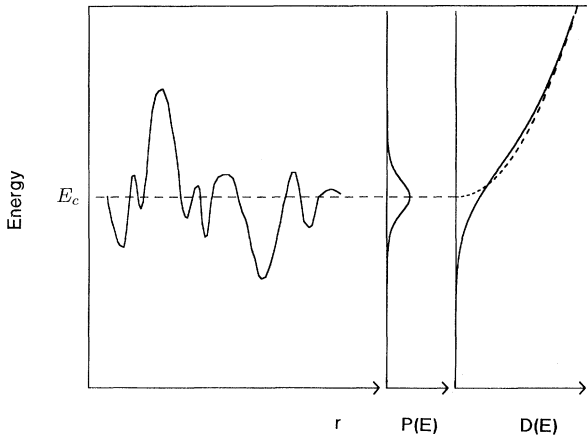


FIG. 4. Full line: Behavior of the conduction-band edge under the influence of a fluctuating potential in a heavily doped semiconductor, distribution function $P(E)$ of the different values of E_c , and the corresponding broadened 3D density of states $D(E)$ according to the Kane model. Dashed line: density of states of an unperturbed semiconductor.

with

$$D_i^{(2)}(E) = \frac{m_i}{\pi \hbar^2} \sum_{\mu} \Theta(E - E_{\mu}^i). \quad (13)$$

We use for all subbands of one carrier type the same broadening parameter ΔV_i . One example is shown in Fig. 5.

The self-consistent calculation of energy levels, wavefunctions, and potential yields nearly the same results, only the quasi-Fermi-levels Φ_n and Φ_p change signifi-

cantly. In order to calculate the spontaneous emission rate $\bar{R}_{\text{spont}}(\hbar\omega)$ it is necessary to know whether the \mathbf{k}_{\parallel} selection rule still applies or not. From our discussion in the Introduction one expects that it will not apply for the very tail states, whereas it may perhaps be a good approximation for higher energies. In the present study we have disregarded this problem and have implicitly assumed \mathbf{k}_{\parallel} conservation by replacing the energetic δ function by the appropriate distribution function of Eq. (10),

$$\begin{aligned} \bar{R}_{\text{spont}}(\hbar\omega) \propto & \int d\epsilon_n \int d\epsilon_p \delta[\hbar\omega - (\epsilon_n - \epsilon_p)] f(\epsilon_n - \Phi_n) [1 - f(\epsilon_p - \Phi_p)] \\ & \times \sum_{h=\text{lh, hh}} |P_{\text{el},h}|^2 \sum_{\mu\nu} |\langle \text{el}, \mu | h, \nu \rangle|^2 \\ & \times \sum_{\mathbf{k}_{\parallel}} P_U(\epsilon_n - E_{\mu}^{\text{el}}(\mathbf{k}_{\parallel}), \Delta E_{\text{el}}) P_U(\epsilon_p - E_{\nu}^h(\mathbf{k}_{\parallel}), \Delta E_h), \end{aligned} \quad (14)$$

with

$$\begin{aligned} E_{\mu}^{\text{el}}(\mathbf{k}_{\parallel}) &= E_{\mu}^{\text{el}} + \frac{\hbar^2 k_{\parallel}^2}{2m_{\text{el}}}, \\ E_{\nu}^h(\mathbf{k}_{\parallel}) &= E_{\nu}^h - \frac{\hbar^2 k_{\parallel}^2}{2m_h}, \quad h = \text{lh, hh}. \end{aligned} \quad (15)$$

In the presence of the δ function the integrals can be carried out and the expression may be transformed to Eq. (1).

The theoretical luminescence spectra shown in Fig. 6 have been numerically calculated by using Eq. (14). For the calculation of ΔV_i the corrected design parameters (which we got from conductance measurements¹⁹) $n_D = 4.25 \times 10^{18} \text{ cm}^{-3}$ and $n_A = 9.75 \times 10^{18} \text{ cm}^{-3}$ and the

layer thicknesses given in Sec. II have been used. These spectra are compared with the experimentally observed ones for the corresponding excitation levels ranging from very low to very high values.

IV. DISCUSSION

The theoretical spectra resulting from our simple model describe the general form of the experimental spectra surprisingly well, especially in comparison with the idealized ones shown in Fig. 3. The broadening leads to smooth spectra in which the subband structure is obscured. The high energy tails of the theoretical spectra fit the experimental ones particularly well, whereas the

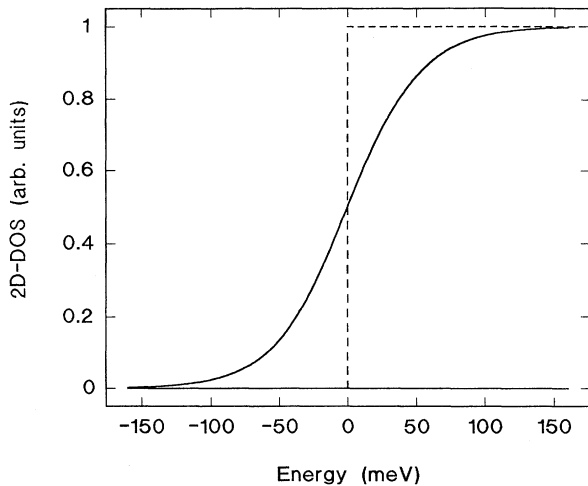


FIG. 5. Full line: Broadened 2D density of states according to the modified Kane model described in the text. The DOS corresponds to an electron subband with a broadening parameter ΔV_{el} of 27 meV and an excitation density $n^{(2)}$ of $4 \times 10^{11} \text{ cm}^{-2}$. Dashed line: Steplike density of states of an unperturbed 2D subband.

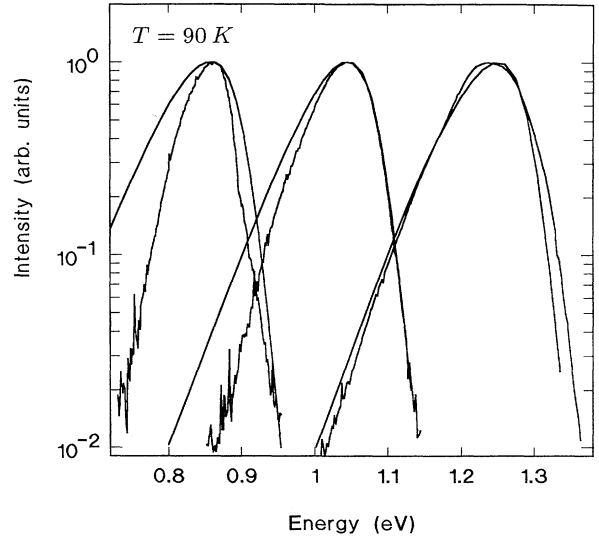


FIG. 6. Calculated spectra for three different excitation densities ($n^{(2)} = 4 \times 10^{11} \text{ cm}^{-2}$; $1.8 \times 10^{12} \text{ cm}^{-2}$; $3.8 \times 10^{12} \text{ cm}^{-2}$) including the broadening mechanism described in the text, in comparison with the corresponding experimental spectra.

agreement for the low energy tail degrades at decreasing degrees of excitation.

The agreement for the high energy tail confirms that the self-consistent calculation of the potential, the energy levels, and the wave functions leads to a correct basis for the description of the properties of *n-i-p-i* structures. In this case, the increasing overlap for higher energy levels is demonstrated. It also demonstrates that for transitions from states with a kinetic energy well above the subband level, the overlap matrix elements are basically constant, as assumed in the theory.

For the spectra at high excitation the agreement between theory and experiment is very good on the low energy side as well. We attribute this to the decreasing modulation of the conduction and valence band and the resulting widening of nearly neutral bulklike *n*- and *p*-doped regions. Thus our assumption of 3D screening seems justified. We note that the low energy tail of the spectra is nearly exponential, as expected from theory. For lower degrees of excitation we expect a less efficient screening of the potential fluctuations compared with the neutral doped bulk material. This should result in a broadening on the low energy side of the luminescence spectra. The experiments, however, exhibit the opposite behavior. This finding can be explained qualitatively in the following way. The deep tail states are expected to be more strongly localized in the *z* direction than the corresponding subband states. This reduces their dipole matrix elements for interband recombination and, therefore, the low energy contributions to the spectra. This effect becomes more and more important at low excitation levels where the electron-hole tunneling recombination occurs over increasingly long distances. This narrowing effect, apparently, overcompensates the widening effect discussed above. However, we have not yet been able to include these effects quantitatively.

Our model allows us to understand why no signature of the 2D subbands has been observed in the luminescence spectra of *n-i-p-i* structures, although it could clearly be demonstrated in other investigations as mentioned in the Introduction. We want to note that the subband spacing $\Delta E_{01}^{\text{el}} = E_1^{\text{el}} - E_0^{\text{el}}$ and the broadening factor ΔV_{el} scale with nearly the same power of the doping density. While the former increases $\propto n_D^{1/2}$ (for empty subbands), the latter increases $\propto n_D^{7/12}$, if one assumes a boxlike carrier distribution which compensates for the impurity charge in the center of the layers (in contrast to the former assumption of a uniform distribution over the respective layer which would produce a power dependence nearer to 1/2). For $n_D = 10^{18} \text{ cm}^{-3}$, e.g., we obtain $\Delta E_{01}^{\text{el}} = 40 \text{ meV}$ and $\Delta V_{\text{el}} = 20 \text{ meV}$, respectively. Thus the ratio $\Delta V_{\text{el}}/\Delta E_{01}^{\text{el}} = 0.5(n_D/10^{18} \text{ cm}^{-3})^{1/12}$, which is important for the question of whether the 2D subband structure is visible in the luminescence spectra, does not change significantly within the whole range of reasonable doping densities. Although $\Delta V_{\text{el}}/\Delta E_{01}^{\text{el}} < 1$, the observation of the signature of the subbands is further obscured by the fact that the contributions from higher subbands to the luminescence are much stronger because of the exponentially increasing overlap of the envelope wave functions. Thus, the exponential tail of a transition associ-

ated with the subband gap $E_{\mu+1}^{\text{el}} - E_{\nu}^h$ may still dominate over the contributions corresponding to the subband gap $E_{\mu}^{\text{el}} - E_{\nu}^h$ at a given photon energy.

This argument holds only for the case of uniformly doped *n-i-p-i* structures. The situation is more favorable for δ -doped *n-i-p-i* systems, for which the observation of 2D subbands in luminescence and absorption experiments has been claimed.⁶

Finally, we point out, that the chances for the observation of transitions corresponding to different subbands are expected to be best for the high energy tail at elevated temperatures. In this regime the competition between the exponential decrease of the carrier density in higher subbands and the exponential increase of overlap will result in more or less equal recombination rates. Therefore, their contributions to the luminescence have about the same weight. This situation is analogous to hetero-*n-i-p-i* structures where such transitions have clearly been resolved.^{20,21}

V. CONCLUSIONS

We have demonstrated that the luminescence from *n-i-p-i* doping superlattices can be modeled quite well by introducing a broadened 2D DOS, which is calculated by applying the Kane model to a 2D subband system. With this simple model we have been able to describe the general features of the luminescence spectra without using any fit parameter. Further experimental and theoretical investigations, including δ -doped structures, are in progress with the goal to refine the model of the screening and to take into account the influence of the potential fluctuations on the wave functions.

ACKNOWLEDGMENT

We want to thank the Deutsche Forschungsgemeinschaft (DFG, Bonn, Germany) for financial support.

APPENDIX

The potentials of the randomly distributed doping atoms cause local variations of the space charge potential in the host material. By means of the statistical method of Holtmark¹⁵ it is possible to calculate a probability distribution of the space charge potential around its original value by looking at a large number of doping atoms.

The total potential $V(\mathbf{r})$ results from a superposition of all the single potentials $v(\mathbf{R}_j)$ of the atoms at the positions \mathbf{R}_j

$$V(\mathbf{r}) = \sum_j v(\mathbf{R}_j) = \frac{e^2}{4\pi\epsilon\epsilon_0} \frac{1}{|\mathbf{r} - \mathbf{R}_j|}. \quad (\text{A1})$$

The probability $P(\epsilon)$ of having a potential energy ϵ is

$$P(\epsilon) = \langle \delta(\epsilon - V) \rangle \quad (\text{A2})$$

with

$$\langle \dots \rangle = \frac{1}{\Omega^N} \prod_{j=1}^N \int dR_j \dots \quad (\text{A3})$$

Here Ω is the volume and N the number of the impurities. Using the integral representation of the δ function, one gets

$$\begin{aligned} \langle e^{-is \sum_j v(R_j)} \rangle &= \left\langle \prod_j e^{-isv(R_j)} \right\rangle \\ &= \frac{1}{\Omega^N} \int dR_1 \dots \int dR_N \left(\prod_j e^{-isv(R_j)} \right) \\ &= \frac{1}{\Omega} \int e^{-isv(R_1)} dR_1 \dots \frac{1}{\Omega} \int e^{-isv(R_N)} dR_N \\ &= \left(\frac{1}{\Omega} \int e^{-isv(R)} dR \right)^N \\ &= \left(1 + \frac{1}{\Omega} \int (e^{-isv(R)} - 1) dR \right)^N. \end{aligned} \quad (\text{A5})$$

For large numbers of N this can be written as an exponential function

$$\lim_{N \rightarrow \infty} \left(1 + \frac{1}{\Omega} c \right)^N = e^{nc} \quad (\text{A6})$$

with

$$\begin{aligned} n &= \frac{N}{\Omega} \quad \text{const} \\ c &= \int (e^{-isv(R)} - 1) dR. \end{aligned}$$

This can be summarized as follows:

$$\lim_{N \rightarrow \infty} \langle e^{-is \sum_j v(R_j)} \rangle = \exp \left(n \int (e^{-isv(R)} - 1) dR \right). \quad (\text{A7})$$

Using the series representation for e^{-isv} one finally gets a general formula of the probability distribution

$$\begin{aligned} P(\varepsilon) &= \frac{1}{2\pi} \int ds e^{is\varepsilon} \\ &\times \exp \left(n \sum_{m=1}^{\infty} \frac{(is)^m}{m!} \int_{\Omega} (v(R))^m d^{\nu} R \right). \end{aligned} \quad (\text{A8})$$

Here ν is the dimensionality of the considered system. As mentioned before we assumed that the carrier systems are nearly three-dimensional, i.e., $\nu = 3$. Using the Yukawa potential for the screened impurities and assuming isotropy, the integrations can be carried out

$$\begin{aligned} P(\varepsilon) &= \left\langle \frac{1}{2\pi} \int ds e^{is\varepsilon} e^{-is \sum_j v(R_j)} \right\rangle \\ &= \frac{1}{2\pi} \int ds e^{is\varepsilon} \langle e^{-is \sum_j v(R_j)} \rangle. \end{aligned} \quad (\text{A4})$$

The exponential function with the sum in the exponent can be written as a product of N exponential functions. As a consequence the N -dimensional integration breaks into N one-dimensional integrations

$$V(R) = \frac{e^2}{4\pi\varepsilon\varepsilon_0 R} e^{-R/L_s}, \quad (\text{A9})$$

$$\int d^3 R = 4\pi \int R^2 dR. \quad (\text{A10})$$

This gives for the first moment of the distribution

$$P_1(\varepsilon) = \frac{1}{\sqrt{2\pi}} \int e^{is\varepsilon} e^{-is\varepsilon_1} ds = \delta(\varepsilon - \varepsilon_1) \quad (\text{A11})$$

with

$$\varepsilon_1 = \frac{e^2}{\varepsilon\varepsilon_0} n L_s^2, \quad (\text{A12})$$

and for the second moment

$$P_2(\varepsilon) = \frac{1}{\sqrt{2\pi}} \int e^{is\varepsilon} e^{-s^2 \varepsilon_2^2 / 2} ds = \frac{1}{\sqrt{2\pi\varepsilon_2}} e^{-\varepsilon^2 / 2\varepsilon_2^2} \quad (\text{A13})$$

with

$$\varepsilon_2 = \frac{q^2}{4\pi\varepsilon\varepsilon_0} (2\pi n L_s)^{1/2}. \quad (\text{A14})$$

The first moment represents the result from the homogeneous background which we must ignore, because we have considered it already as the n - i - p - i potential. We are only interested in the fluctuating part of the potential which is represented by the second moment [Eq. (A13)]. As mentioned in the text, this distribution is only applicable at very high doping concentrations which are not reached in our case. We used another distribution with an appropriate width, introduced by Unger, which is described in the text.

- ¹G.H. Döhler, CRC Crit. Rev. Solid State Mater. Sci. **13**, 97 (1987).
- ²G.H. Döhler and K. Ploog, in *Synthetic Modulated Structure Materials*, edited by L.L. Chang and B.C. Giessen (Academic Press, New York, 1985), p. 163.
- ³G.H. Döhler, H. Künzel, D. Olego, K. Ploog, P. Ruden, H.J. Stolz, and G. Abstreiter, Phys. Rev. Lett. **47**, 864 (1981).
- ⁴Ch. Zeller, G. Abstreiter, and K. Ploog, Surf. Sci. **142**, 456 (1977).
- ⁵J.C. Maan, Th. Englert, H. Künzel, A. Fischer, and K. Ploog, Solid State Commun. **47**, 383 (1983).
- ⁶E.F. Schubert, T.D. Harris, J.E. Cunningham, and W. Jan, Phys. Rev. B **39**, 11 011 (1989).
- ⁷E.F. Schubert, B. Ullrich, T.D. Harris, and J.E. Cunningham, Phys. Rev. B **38**, 8305 (1988).
- ⁸K. Unger, *Semiconductor Optoelectronics* (PWN-Polish Scientific Publishers, Warszawa, 1980).
- ⁹A. Gold, J. Serre, and A. Ghazali, Phys. Rev. B **37**, 4589 (1988).
- ¹⁰G. Döhler, in *Properties of Impurity States in n-i-p-i Superlattice Structures*, edited by G.H. Döhler, C.Y. Fong, I.P. Batra, and S. Ciraci, *NATO Advanced Study Institute Series B: Physics* (Plenum, New York, 1988), p. 159.
- ¹¹C. Metzner, H.J. Beyer, and G.H. Döhler, Phys. Rev. B **46**, 4128 (1992).
- ¹²J.D. Bruno and P.P. Ruden, SPIE Proc. **792**, 50 (1987).
- ¹³H.J. Beyer, C. Metzner, J. Heitzer, and G.H. Döhler, Superlatt. Microstruct. **6**, 3 (1989).
- ¹⁴E.O. Kane, Phys. Rev. **131**, 79 (1963).
- ¹⁵J. Holtsmark, Ann. Phys. **58**, 577 (1919).
- ¹⁶R. Schwabe, A. Haufe, H. Fieseler, and K. Unger, J. Phys. C **21**, 2951 (1988).
- ¹⁷B.I. Halperin and M. Lax, Phys. Rev. **148**, 722 (1966).
- ¹⁸K. Unger, Phys. Status Solidi B **149**, K141 (1988).
- ¹⁹M. Renn, Ph.D. thesis, Universität Erlangen, 1991.
- ²⁰R.A. Street, G.H. Döhler, J.N. Miller, R.D. Burnham, and P.P. Ruden, in *Proceedings of the 18th International Conference on the Physics of Semiconductors*, edited by O. Engström (World Scientific, Singapore, 1987), p. 215.
- ²¹R.A. Street, G.H. Döhler, J.N. Miller, and P.P. Ruden, Phys. Rev. B **33**, 7043 (1986).